RSC Advances

PAPER

View Article Online
View Journal | View Issue

Check for updates

Cite this: *RSC Adv.*, 2022, **12**, 14945

Comparing the efficacy of various methods for sulfate radical generation for antibiotics degradation in synthetic wastewater: degradation mechanism, kinetics study, and toxicity assessment†

Ali Behnami,[ab] Ehsan Aghayani,[c] Khaled Zoroufchi Benis,[d] Mohammad Sattari[e] and Mojtaba Pourakbar *[a]

In the present study the aim was to investigate and compare various activation processes for amoxicillin degradation. UV radiation, ultrasound, heat, and hydrogen peroxide were selected as the persulfate activation methods. The effects of various parameters such as pH, persulfate concentration, reaction time, AMX concentration, radical scavengers, and anions were thoroughly investigated. The results showed that AMX degradation was following the pseudo-first order kinetic model. The reaction rate of 0.114 min^{-1} was calculated for the UV/PS process, which was higher than that of the other investigated processes. The AMX degradation mechanism and pathway investigations revealed that sulfate and hydroxyl radicals were responsible for the degradation of AMX by two degradation pathways of hydroxylation and the opening of the β-lactam ring. Competition kinetic analysis showed that the second-order rate constant of AMX with sulfate radicals was 8.56×10^9 L mol^{-1} s^{-1} in the UV/PS process. Cost analysis was conducted for the four investigated processes and it was found that 1.9 $\$m^{-3}$ per order is required in the UV/PS process for the complete destruction of AMX. Finally, cytotoxic assessment of the treated effluent on human embryonic kidney cells showed a considerable reduction in AMX-induced cell cytotoxicity, proving that the investigated process is sufficiently capable of completely destroying AMX molecules to nontoxic compounds. Therefore, it can be concluded that UV radiation is much more effective than other methods for persulfate activation and can be considered as a reliable technique for antibiotic removal.

Received 12th March 2022
Accepted 12th May 2022

DOI: 10.1039/d2ra01618d

rsc.li/rsc-advances

Open Access Article. Published on 18 May 2022. Downloaded on 12/27/2025 9:06:54 AM.
This article is licensed under a Creative Commons Attribution-NonCommercial 3.0 Unported Licence.

1. Introduction

During the late last century, industrialization and population growth have caused the emergence of several organic micro-pollutants in the environment, such as pharmaceutical drugs and personal care products, some of which are classified as persistent and non-biodegradable compounds.[1] Antibiotics have been gaining more attention among pharmaceuticals considering their widespread use in human and veterinary medicine. Even at low concentrations, antibiotics can have negative effects on aquatic environments in terms of their toxicity, low biodegradability, and high chemical oxygen demand.[2] Moreover, the contribution of antibiotics in emerging "Antibiotic Resistance" is also a matter of concern to modern human and veterinary medicine.[3] Amoxicillin (AMX), a β-lactam antibiotic, is one of the top ten most prescribed antibiotics worldwide, belonging to the semi-synthetic penicillin.[4] AMX is a widely used antibiotic in human and veterinary medicine to treat a number of bacterial infections. Due to its poor absorption in both human and livestock body, a large quantity of consumed AMX is excreted mainly through urine and feces into the wastewater system.[5] AMX is a potential threat to the environment, human and animal lives, since it gives rise to antibiotic resistance genes and beta-lactam resistant bacteria.[4,6] AMX has been detected at μg L^{-1} concentrations in the influent and fluent of wastewater treatment plants and also surface water,[7,8] while its levels in pharmaceutical industry effluents may reach mg L^{-1} concentrations.[9] Hence, antibiotic containing

[a]*Department of Environmental Health Engineering, Maragheh University of Medical Sciences, Maragheh, Iran. E-mail: ppourakbar@yahoo.com; Tel: +98 04132726363*
[b]*Department of Environmental Health Engineering, Iran University of Medical Sciences, Tehran, Iran*
[c]*Research Center for Environmental Contaminants (RCEC), Abadan University of Medical Sciences, Abadan, Iran*
[d]*Department of Chemical and Biological Engineering, University of Saskatchewan, Saskatoon, Saskatchewan, Canada*
[e]*Department of Biophysics, Faculty of Biological Sciences, Malayer University, Malayer, Iran*

† Electronic supplementary information (ESI) available. See https://doi.org/10.1039/d2ra01618d

© 2022 The Author(s). Published by the Royal Society of Chemistry

Open Access Article. Published on 18 May 2022. Downloaded on 12/27/2025 9:06:54 AM. This article is licensed under a Creative Commons Attribution-NonCommercial 3.0 Unported Licence.

streams should be effectively treated in order to mitigate their abovementioned detrimental impacts on the environment and living organisms.

Biological treatment systems cannot efficiently remove all antibiotics, as most of the antibiotics are not easily biodegradable, and these systems only target biodegradable antibiotics.[10] On the other hand, although some disinfection technologies such as ozonation,[11] chlorination,[12] and bromination[13] have been investigated for their influence on antibiotics degradation in polluted waters, the formation of secondary toxic pollutants undermine their application.

Considering the drawbacks of conventional treatment technologies, advanced oxidation processes (AOPs) can be considered a promising alternative for efficiently removing antibiotics from wastewater. AOPs could generate non-selective oxygen-based oxidizers mainly hydroxyl or sulfate radicals ($OH^{\bullet}$ and $SO_4^{\bullet-}$) for degradation and mineralization of target compounds.[14] To date, various AOPs such as UV/H_2O_2,[5,15] UV/catalyst,[16] O_3/UV,[17] UV/PS,[18] vacuum ultraviolet (VUV)[19] PS/catalyst,[3] Fenton reactions,[6] photo-Fenton,[20] electro-oxidation,[4] and sonochemical degradation[2] have been studied for degradation of AMX in aqueous solutions.

AOPs can be classified as either $SO_4^{\bullet-}$-based AOPs or $OH^{\bullet}$-based AOPs based on radical species. Recently, $SO_4^{\bullet-}$-based AOPs attracted significant attention in comparison to $OH^{\bullet}$-based AOPs because of their higher selectivity, longer half-life of 30–40 μs, and higher redox potential of 2.5–3.1 V. Relatively higher selectivity of sulfate radical than that of hydroxyl radical is due to the strong oxidizing power of sulfate than hydroxyl radical.[21] Moreover, in case of antibiotics removal from contaminated waters, it has been proved that sulfate radicals show more efficient antibiotic activity removal against sulfur-containing β-lactam antibiotics such as AMX and penicillin.[22] Therefore, $SO_4^{\bullet-}$-based AOPs may be a promising alternative for $OH^{\bullet}$-based AOPs in treating antibiotic-containing wastewaters.

Sulfate radicals can be generated by activating persulfate (PS) or peroxymonosulfate (PMS) in the presence of metal or non-metal catalysts, energy (such as ultrasound, microwave, visible light, UV, and heat), alkali activation, and carbon.[23,24] However, limited studies have investigated the efficacy of PS activating methods for the degradation of AMX, including PS/catalyst,[3] UV/PS,[5] heat/PS,[23] and ultrasound (US)/PS.[25] This is the first comprehensive report evaluating various methods of activating PS for AMX degradation in aqueous solutions.

Accordingly, the present study aimed to evaluate the efficacy of different methods for activating persulfate, including H_2O_2/PS, UV/PS, heat/PS, US/PS, and Alkali/PS for the degradation and mineralization of AMX in synthetic wastewater. The effects of different process variables, including pH, PS concentration, reaction time, the initial concentration of antibiotic, radical scavengers, and anions, were investigated on the performance of the abovementioned processes. In addition, the decomposition mechanism of the final products resulting from AMX degradation has been thoroughly investigated. The detoxification of AMX containing synthetic wastewater was also determined. The findings of the present study could provide useful information to establish an appropriate strategy for the treatment of AMX containing streams.

2. Materials and methods

2.1. Materials and reagents

The AMX solution was freshly prepared daily using AMX ($C_{16}H_{19}N_3O_5S$) powder and distilled water. The pure AMX powder (100%) was purchased from a local pharmaceutical company. The AMX solution pH was adjusted by sodium hydroxide and acid sulfuric normal solutions. All the consumed chemicals in the present study were high quality of analytical grade chemicals and were bought from Merck Co.

2.2. Experimental set-ups

In the present study, 4 different reactors with different configurations were used. All the reactors had a working volume of 250 mL. The sonochemical reactions were taken place using an ultrasound bath. For the investigation of the effect of heat/PS, the hotplate coupled with a thermosensor was used to adjust the solution temperature.

The UV photoreactor had a 9 W UVC lamp separated from the solution by a quartz sleeve. The solution was injected from the bottom of the photoreactor and the reaction took place in an upflow mode. The content of the UV photoreactor was circulated using a peristaltic pump with a flow rate of 0.2 L min^{-1}. In addition, an outer layer was also used to control the process temperature by water circulation. The photoreactor temperature was constantly controlled and maintained at 25 °C during the reaction time.

2.3. Experimental procedure

Different oxidation mechanisms, either alone or combined, were thoroughly studied. First, the effect of different chemicals and operational conditions such as persulfate alone, hydrogen peroxide alone, UV radiation, ultrasonication, and heat were investigated for the AMX degradation to find the contribution of sole oxidation agents in AMX degradation. In the second stage of the study, the AMX degradation was investigated by different activation methods of PS. The effects of operating conditions such as PS activator concentration, PS concentration, solution pH, reaction time, and AMX concentration were thoroughly investigated in H_2O_2/PS, UV/PS, heat/PS, and US/PS processes.

The effect of the water matrix was also investigated for AMX degradation. The effect of the presence of anions HCO_3^-, CO_3^{2-}, (Cl^-, NO_3^-, and SO_4^{2-}), tap water, and wastewater treatment plant effluent were investigated on AMX degradation. *tert*-Butanol (TBA), and benzene were also used as the hydroxyl and sulfate radical quenchers to find the main radical species. All the experiments were conducted in duplicate.

2.4. Analytical methods

Agilent HPLC coupled with C18 column (3.5 μm, 4.6 × 100 mm) and a UV detector (wavelength of 190 nm) was used for AMX detection. Acetonitrile and phosphate buffer (pH = 4.8) with

© 2022 The Author(s). Published by the Royal Society of Chemistry

Open Access Article. Published on 18 May 2022. Downloaded on 12/27/2025 9:06:54 AM.
This article is licensed under a Creative Commons Attribution-NonCommercial 3.0 Unported Licence.

a volumetric ration of 40/60 and flow rate of 0.5 mL min^{-1} was applied for AMX separation in the solutions.

Liquid chromatography/mass spectrometry (LC/MS) of Quartro Micro API micromass Waters 2695 was used to detect by-products of AMX degradation. Chromatography column of zorbax Sb-C18 (2.1 × 100 mm, 3.0 μm particle size) was used at ambient temperature. 10 μL sample was injected in each run. Isocratic mode at a flow rate of 0.2 mL min^{-1} was set to the mobile phase of 96% water with 0.1% formic acid, and 4% methanol. For the MS operation, the positive electrospray ionization (ESI) with an m/z ranging from 50 amu to 2000 amu was applied. Nitrogen gas at a flow rate of 300 L h^{-1} was used as the nebulizer and desolvation gas. The Jet Stream conditions were applied with capillary voltage of 4 kV, extractor of 3 V, fragment voltage of 35 V, nebulizer pressure of 50 psi, and gas temperature of 250 °C.

2.5. Toxicity assessment

Human embryonic kidney cells (HEK 293) were used for cytotoxicity assessment. The cells were obtained from National Cell Bank of Iran (NCBI). They were cultured at 37 °C and 5% CO_2 in Dulbecco's Modified Eagle Medium (DMEM) supplemented with 10% heat-inactivated fetal bovine serum. Then, cells were harvested by trypsinization and seeded in complete medium in 96-well tissue culture plates at a density of 104 cells in 100 μL media per well and incubated during the day at 37 °C, and 5% CO_2. After 24 h of incubation, the toxicity of the AMX inflow and outflow solutions with different AMX concentrations were investigated by replacing the new media with culture media. Cells treated with medium only attended as a control group, and cells were incubated for 24 and 48 h. Separately, MTT stock (3-[4,5-dimethylthiazol-2-yl]-2,5-diphenyltetrazolium bromide) was prepared by dissolving 5 mg of MTT per ml of PBS. Then, it was filtered through a 0.22 μm filter before diluting with DMEM at the concentration of 10% v/v. Succinate dehydrogenase is able to convert MTT to an insoluble purple formazan in the mitochondria of live cells. MTT (5 mg mL^{-1}) solution was then added to each well, and the cells were further incubated for 4 h.

Afterward, the discarded supernatant and 100 μl of DMSO were added to each well and mixed for dissolution of the crystals. Then, the color intensity was measured by BioTek ELx808 microplate reader at a wavelength of 540 nm. The number of viable and metabolically active cells at this stage is directly proportional to the amount of generated purple color.

3. Results and discussion

3.1. Contribution of sole oxidation processes

The influence of various sole oxidation processes, including PS, H_2O_2, UV, heat, and US was investigated for the degradation of AMX. Fig. 1 illustrates the contribution of different oxidation processes in AMX oxidation. As shown to Fig. 1, AMX was slightly removed in direct UV, US, and PS systems, and AMX removal efficiency in these systems was calculated about 8.4, 11.6, and 11%, respectively, at 60 min of reaction time. However, H_2O_2 alone showed the highest AMX removal efficiency among the different oxidation processes achieving a 32.2% AMX removal efficiency at 60 min of reaction time.

H_2O_2 alone acts as a strong oxidant (redox potential of 1.76 V) capable of degrading a wide range of inorganic and organic contaminants, especially in acidic conditions. However, in

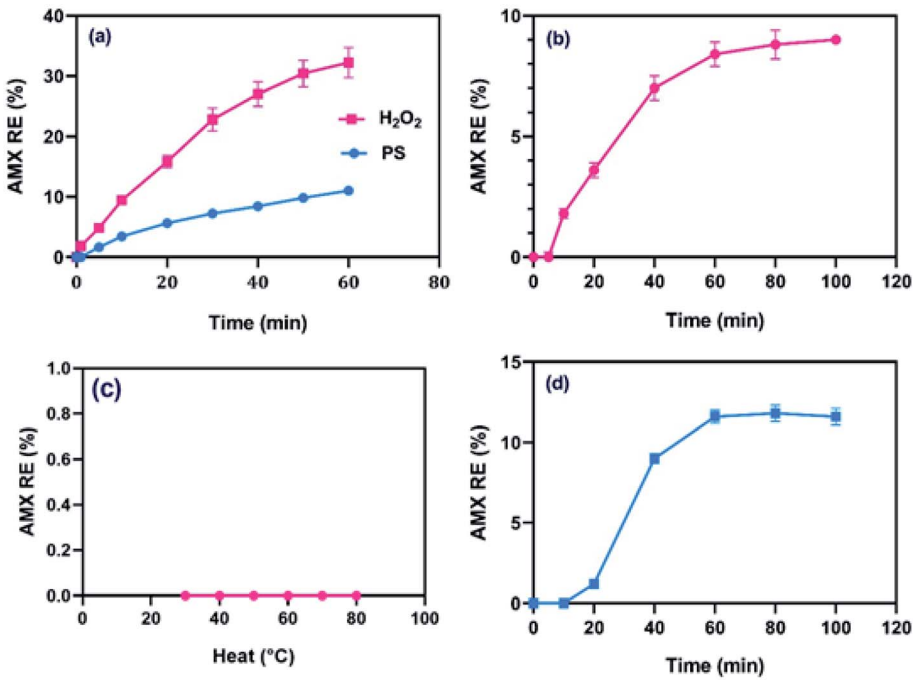

Fig. 1 Contribution of PS, H_2O_2 (a), UV (b), heat (c) and US (d) on AMX removal. Experimental conditions: AMX concentration = 50 mg L^{-1}, PS concentration = 1 mM, H_2O_2 concentration = 1 mM, US = 30 kHz, pH = 7.

Open Access Article. Published on 18 May 2022. Downloaded on 12/27/2025 9:06:54 AM.
This article is licensed under a Creative Commons Attribution-NonCommercial 3.0 Unported Licence.

alkaline conditions, H_2O_2 production efficiency decreases as a result of decreasing in hydro peroxide ions (HO_2^-).[26]

PS also has high redox potential (2.01 V); however, PS alone showed negligible contribution in AMX removal that can be attributed to the lack of PS activating agents, which cause PS to remain almost intact in the solution. This is consistent with the reported results in previous investigations.[21,27]

In this study, the optimum time for degrading 50 mg L^{-1} AMX applying the US alone with 30 kHz power was obtained around 60 min above which no significant effect on AMX degradation was observed.

The effect of US in AMX degradation can be explained by the acoustic cavitation phenomena, in which US power increases the number of cavities generated. Inside the cavitation bubbles, thermal dissociation of water vapor and oxygen molecules causes the generation of various highly reactive radicals, including $H^{\bullet}$, $HO_2^{\bullet}$, and $HO^{\bullet}$, which contribute to AMX degradation.[28] However, maximum degradation rates of AMX by US process can be achieved at optimal US intensity. Because at high US intensities, fewer radicals would be generated due to a high number of gas bubbles generation which scatter the sound waves and prevent the energy from dissipating in the liquid.[29]

UV alone also contributed insignificantly in AMX degradation, reaching 9% removal efficiency after 100 min reaction time. Similar results were obtained for the degradation of ketamine and methamphetamine using UV alone.[30] The main mechanism of compound degradation, when exposed to UV, is photolysis, in which photons break down a chemical substance. However, in a study performed by Elmolla *et al.*,[31] AMX absorbed light below 300 nm, and no significant degradation rate was observed at 365 nm UV irradiation. Therefore, hydrolysis reaction was found the main mechanism for AMX removal through UV irradiation that occurs *via* nucleophile H_2O attack to the β-lactam ring of antibiotic followed by ring opening.[31]

As expected, heat alone was not able for the degradation of AMX, even at elevated temperatures (80 °C), therefore the effect of heating alone on the AMX degradation can be neglected.

3.2. The effect of pH and persulfate activation mechanism

Solution pH as one of the important factors in chemical reactions was investigated in all processes for radical generations. Fig. 2 illustrates the effect of pH on the process performance. In all the experiments conducted for the effect of pH, the AMX concentration was 140 μM, and PS was 1 mM. As shown in the figure, persulfate activation by hydrogen peroxide is not dependent on solution pH, and almost the same removal efficiencies are observed for AMX degradation. However, AMX removal is obviously affected in UV/PS, US/PS, and heat/PS processes.

In the H_2O_2/PS process, the radical generation mechanism initially starts with the formation of hydroxyl radical as a result of hydrogen peroxide decomposition, and in the next step, persulfate activation by hydroxyl radical leads to the generation of sulfate radicals.[32] Furthermore, the solution temperature was monitored during the reaction. An increase in the solution temperature was observed, which could also be a further factor

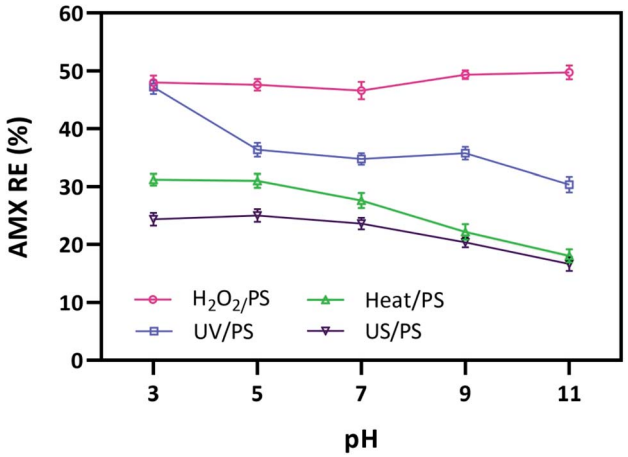

Fig. 2 The effect of pH on PS activation in H_2O_2/PS ([H_2O_2] = 1 mM, time = 30 min), UV/PS (time = 15 min), heat/PS (T = 60 °C, time = 30 min), US/PS (US intensity = 30 kHz, time = 30 min).

for persulfate activation in the H_2O_2/PS process. Higher concentrations of hydrogen peroxide in the presence of persulfate leads to the increase of solution temperature. The heat resulted from the decomposition of hydrogen peroxide. Hilles *et al.*[32] also reported a temperature increase in the H_2O_2/PS process. Therefore, higher solution temperature and the hydrogen peroxide presence in the solution lead to higher radical generation, which is observed by a slight increase in the AMX removal efficiency in the H_2O_2/PS process.

On the other hand, AMX removal increased significantly in the acidic condition, revealing that lower pH values are favorable for AMX destruction. As shown Fig. 2, alkaline condition reduces the sulfate radical production leading to less effective degradation of AMX. Lower radical concentrations in persulfate activation have also been reported in the literature. Zhang *et al.*[33] investigated the degradation of three pharmaceutical compounds (sulfamethoxazole, trimethoprim and N4-acetyl-sulfamethoxazole) using UV/PS process. They have also confirmed that lower radical concentrations are present in alkaline conditions. Jiang *et al.*[34] investigated ciprofloxacin degradation using a thermally activated persulfate process. They also found that acidic condition is favorable for ciprofloxacin degradation. Following mechanisms can be proposed for persulfate activation under acidic conditions:

I. The activation pathway of persulfate in alkaline conditions, as given in eqn (1) shows that only one sulfate radical is generated per two persulfate molecules.[14,35] While the activation mechanisms of persulfate using UV radiation, ultrasound, and heat are quite different from that of base-activated persulfate. As shown in eqn (2), two sulfate radicals are generated per persulfate molecules using UV, ultrasound, and heat activation methods.[36,37] Therefore, alkaline conditions inevitably reduce the sulfate radical concentrations, and lower organic contaminant degradation will occur.

$$2S_2O_8^{2-} + 4OH^- \rightarrow SO_4^{\bullet -} + 3SO_4^{2-} + O_2^{\bullet -} + 2H_2O \quad (1)$$

© 2022 The Author(s). Published by the Royal Society of Chemistry

Open Access Article. Published on 18 May 2022. Downloaded on 12/27/2025 9:06:54 AM.
This article is licensed under a Creative Commons Attribution-NonCommercial 3.0 Unported Licence.

$$S_2O_8^{2-} + \text{UV or US or heat} \rightarrow 2SO_4^{\cdot -} \quad (2)$$

II. The species of active radicals differ depending on pH variation. Generally, at neutral and alkaline solutions, sulfate radical can produce hydroxyl radical. Liang and Su[38] reported that sulfate radical is the predominant radical at pH values lower than 7; at pH = 9, both sulfate and hydroxyl radicals are present in the solution and finally and at pH values above 9, hydroxyl radical is the dominant radical species in the solution. Accordingly, the degradation of the organic contaminants will vary as a function of pH. It is reported that the rate constant of AMX with sulfate radical is 2.79×10^9 M^{-1} S^{-1} which is higher than that of hydroxyl radical with AMX (2.02×10^9 M^{-1} S^{-1}).[39]

III. AMX has different ionization states due to different functional groups, including carboxyl ($pK_a = 2.67$), amine ($pK_a = 7.11$), and phenol ($pK_a = 9.55$).[40,41] Therefore, AMX molecules can be cationic, anionic, or neutral at various pH values. Fig. 3 illustrates the ionized structure of AMX at various pH based on pK_a values. As shown in the figure, the density of positive charges over AMX molecules increases at lower pH values by accepting a proton and forming an ion with a positive charge. While at alkaline conditions, AMX loses a proton, forming a negatively charged ion. The positive charge of the AMX increases the electrostatic attraction towards $SO_4^{\cdot -}$. On the other hand, increasing the pH leads to deprotonation of AMX and the formation of negative charges. Consequently, electrostatic repulsion between AMX and $SO_4^{\cdot -}$ increases causing the reduction of AMX degradation.

3.3. Optimization of parameters in the investigated processes

The results of PS/H_2O_2 process are illustrated in Fig. 2. The AMX removal efficiency in the PS/H_2O_2 process is not dependent on the solution pH, and only a slight increase in the AMX removal efficiency is observed which could be due to the fact that alkaline activation of persulfate could also take place in this process.[32] However, due to the negligible increase of removal efficiency (about 3%) the neutral pH was selected to investigate the other parameters. Fig. S1† illustrates the effect of H_2O_2/PS ratio on AMX degradation. The results show that the increase of the H_2O_2/PS ratio leads to the increase of AMX degradation. This ratio was adjusted by keeping the PS concentration at a constant level of 1 mM. As it is shown, the increase of H_2O_2 concentration shows an increasing trend in removal efficiency. The highest AMX removal was observed at H_2O_2/PS ratio of 1.4. In this process, hydrogen peroxide reacts with persulfate to form sulfate and hydroxyl radicals (eqn (3)).[42] In addition, the residual persulfate could also be activated by the present radical species as given in eqn (4).[43]

$$S_2O_8^{2-} + H_2O_2 \rightarrow 2SO_4^{\cdot -} + 2HO^{\cdot} \quad (3)$$

$$HO^{\cdot} + S_2O_8^{2-} \rightarrow HSO_4^{-} + SO_4^{\cdot -} + \frac{1}{2}O_2 \quad (4)$$

Persulfate activation by hydrogen peroxide has been reported in the literature. Hilles *et al.*[32] investigated the performance of the H_2O_2/PS process for the treatment of landfill leachate. They had tested different dosages of hydrogen peroxide and persulfate to find the best performance of the process at H_2O_2/PS ratio of 1.47 : 1. In another study, H_2O_2/PS process was selected for the mineralization of carbamazepine. They have reported that about 20% of the carbamazepine was mineralized after a reaction time of 40 min in H_2O_2/PS ratio of 1.9.[44] Therefore, the optimum H_2O_2/PS ratio of 1.4 in the present study is similar to that of values reported in the literature.

Fig. S2† illustrates the effect of persulfate concentration in the UV/PS process. As it is shown in the figure, AMX degradation is increasing by increasing the persulfate concentration. The higher AMX removal is observed at a persulfate concentration of 0.6 mM, and further increase of the persulfate concentration does not influence the process performance. This is due to the self-scavenging of the generated radicals with themselves and

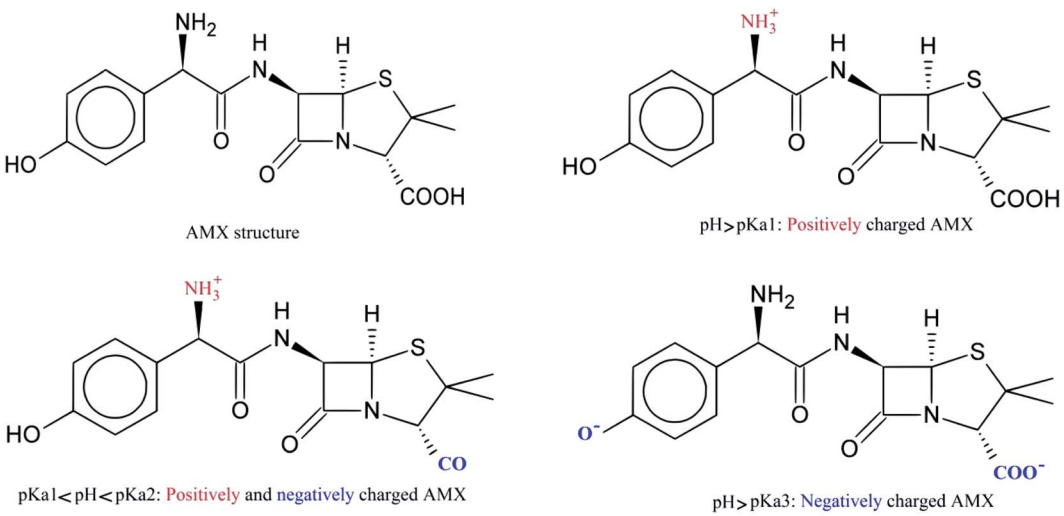

Fig. 3 Ionized structure of AMX molecule at various pH and pK_a of the compound.

Open Access Article. Published on 18 May 2022. Downloaded on 12/27/2025 9:06:54 AM.
This article is licensed under a Creative Commons Attribution-NonCommercial 3.0 Unported Licence.

with the excess persulfate molecules present in the solution.[14] Therefore, 0.6 mM of persulfate was selected as the optimum concentration in the UV-activated persulfate process.

Investigation of the AMX degradation in the presence of higher liquid temperatures and PS concentrations (heat/PS) show that higher temperatures can activate the PS in the solution. As it is shown in Fig. S3,† the higher AMX degradation is reached at PS concentrations of 1.2 mM. In addition, there are higher removal efficiencies at higher temperatures, and the best process performance is observed at 70 °C. These findings are in accordance with the findings of similar studies using heat for PS activation. Liu *et al.*[45] investigated the present process for degradation of sulfachloropyridazine. They have reported that higher temperatures activate the PS molecules, and two sulfate radicals are generated, which can initiate other chemical reactions for various radical generations and contaminant oxidation.

In the last investigated process, PS activation was monitored by ultrasound. Fig. S4† illustrates the effect of various persulfate concentrations in the US/PS process. The results clearly show a synergistic effect in the combination of US and PS compared to the application of PS and US alone. Ultrasound is able to activate persulfate molecules by the breakage of O–O bond, which is due to the cavitation, high temperatures, and pressures.[46] Our study results also show that the highest removal of AMX is observed at a PS concentration of 0.8 g L^{-1}.

3.4. The effect of reaction time and degradation kinetics

In order to directly compare the AMX removal efficiencies in the H_2O_2/PS, UV/PS, heat/PS, and US/PS processes, the kinetics of the AMX degradation were determined by the pseudo-first-order (PFO) kinetic model. The PFO kinetic model can be written as:

$$\ln\left(\frac{C_t}{C_0}\right) = -k_{obs}t \quad (5)$$

where C_0 and C_t are the AMX concentrations (mg L^{-1}) at the beginning and at time t (min) after the reaction started, respectively, and k_{obs} is PFO kinetic model reaction rate constant (min^{-1}), which is obtained from fitting the eqn (5) to the experimental data.

The reaction rate constants of AMX degradation in the four investigated processes with different initial concentrations were summarized in Fig. 4a. The R^2 values for all the models were higher than 0.95, indicating that the PFO model well described the experimental data. The low k_{obs} of direct H_2O_2, PS, UV, US, and heat indicated their insignificant capability to degrade AMX. However, the addition of PS increased the k_{obs} of H_2O_2, UV, US, and heat processes significantly from 6.742×10^{-3} to 0.039, 1.574×10^{-3} to 0.114, 1.504×10^{-3} to 0.030, and 0.000 to 0.023 min^{-1}, respectively. By comparing the reaction rate constants of the four processes, it was observed that the AMX oxidation reaction by UV/PS process was faster than the other three processes (*e.g.*, at AMX initial concentration of 25 mg L^{-1}: 2.9, 3.6, and 4.9 times higher than H_2O_2/PS, US/PS, and heat/PS, respectively). The effect of the initial AMX concentration was also evaluated and compared (Fig. 4a), which showed that the

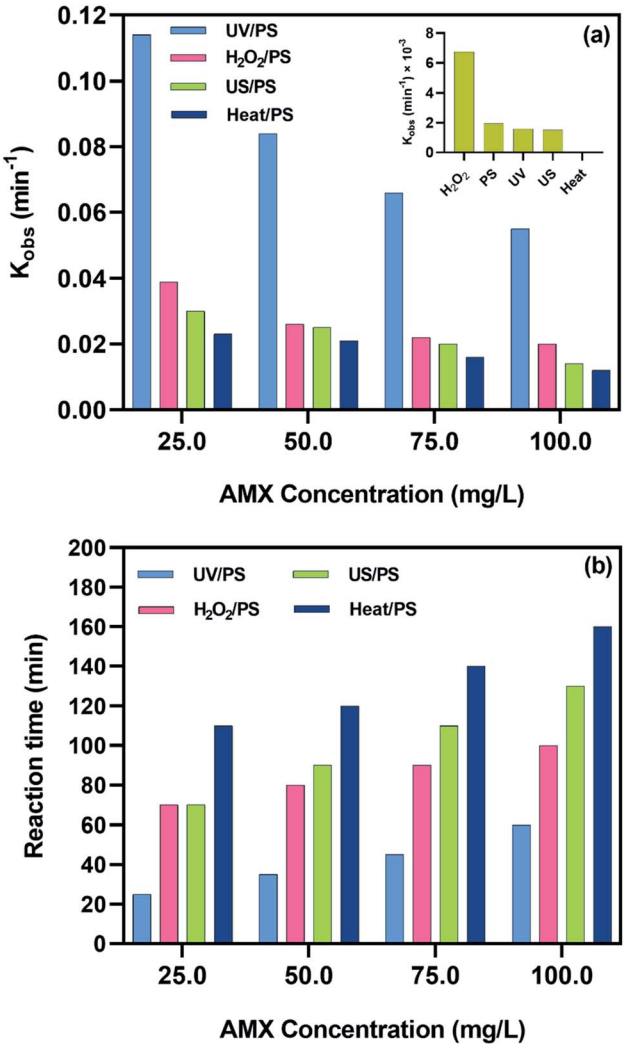

Fig. 4 (a) PFO kinetic model reaction rate constant, and (b) required time to degrade %100 of AMX for H_2O_2/PS, UV/PS, heat/PS, US/PS processes.

rate of AMX degradation is directly proportional to its initial concentration. Accordingly, increasing the initial concentration of AMX prolonged the required time to degrade the whole amount of the AMX (Fig. 4b) with the shortest reaction time for UV/PS process (*e.g.*, at AMX initial concentration of 100 mg L^{-1}: 1.7, 2.2, and 2.7 times higher than H_2O_2/PS, US/PS, and heat/PS, respectively). In addition to the initial concentration of the contaminant, the radical precursor concentration could also influence the k_{obs} values. As it was illustrated in Fig. S2,† the increase of the persulfate concentration increases the AMX removal efficiency, and therefore higher reaction rate constants could be reached at higher persulfate concentrations.

3.5. AMX degradation mechanism and by-products

3.5.1. AMX degradation by-products. The degradation products and intermediates of AMX (50 ppm) during the degradation by UV/PS process were determined by LC-MS in the positive mode $[M + H]^+$. The obtained results at the time

© 2022 The Author(s). Published by the Royal Society of Chemistry

Open Access Article. Published on 18 May 2022. Downloaded on 12/27/2025 9:06:54 AM.
This article is licensed under a Creative Commons Attribution-NonCommercial 3.0 Unported Licence.

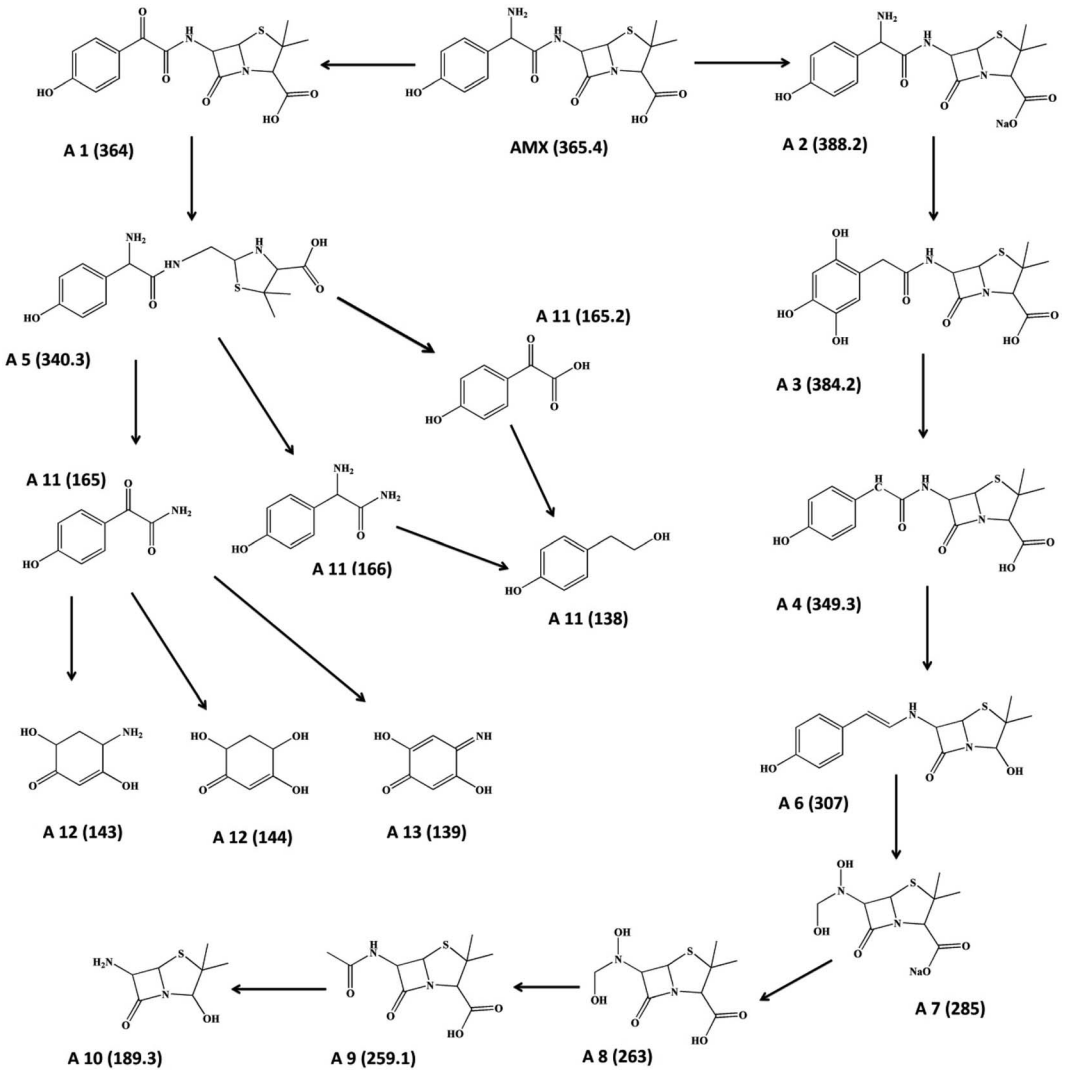

Fig. 5 Degradation pathway of AMX in UV/PS process (AMX concentration: 50 ppm).

intervals of 5, 10, 20, and 40 min are illustrated in Fig. 5 and Table S1.† Based on the results, two potential degradation pathways of (i) hydroxylation and (ii) the opening of the β-lactam ring were proposed. Considering the point that many drugs have aromatic rings in their chemical structures, hydroxylation reactions are typically very common reactions for degradation. These reasons has been approved by finding hydroxyl derivatives in nature due to drug degradation.[47] Based on LC-MS result, hydroxyl groups are added to the AMX molecule at positions more susceptible to an electrophilic attack, such as nitrogen atoms with the lone pair of electrons and the benzoic ring, on the basis of the Frontier Orbital Theory by reaction with sulfate radicals (Li *et al.*, 2019b). The hydroxylation leads to the formation of intermediates A1 (*m*/*z* 364) and A3 (*m*/*z* 384.2). Simultaneity creation of hydroxyl radicals with sulfate lead to oxidation attacks at the regions susceptible to both electrophilic and nucleophilic species, so that after 5 min degradation and release of NH^{4+} and H_2O, in this situation the intermediates A4 (*m*/*z* 349.3) and A6 (*m*/*z* 307) were detected.[48] The detection of A10 (*m*/*z* 189.3), A9 (*m*/*z* 259.1), A8 (*m*/*z* 263), and A7 (*m*/*z* 285) after 20 min degradation is also confirming the point that sulfate and also hydroxyl radicals which are capable of attacking five-membered rings lead to the decarboxylation reactions.[49]

The second scenario for degradation route could be through the destruction of the four-membered β-lactam ring, leading to the formation of intermediate by detect respective hydrolysis by-products corresponds to the penicilloic acid A2 (*m*/*z* 388.2), A3 (*m*/*z* 384.2), and A4 (*m*/*z* 349.3). The attack of sulfate radical to the secondary amine and carbonyl group yields further rearrangement of the molecule. Sulfur atom on the thioether group is susceptible to both hydroxyl and sulfate radical which finally leads to the formation A11–A13.[5] Presence of radical species in the solution especially sulfate radical continuous the degradation reactions leading to the open-chain structures and oxidized to inorganic ions, CO_2, and water. Therefore, complete destruction of AMX molecules to inorganic compounds could be reached at degradation times of above 40 min.

3.5.2. Dominant radical species and the degradation mechanism in the UV/PS process. It has been reported that persulfate activation leads to the generation of sulfate radical as

Open Access Article. Published on 18 May 2022. Downloaded on 12/27/2025 9:06:54 AM.
This article is licensed under a Creative Commons Attribution-NonCommercial 3.0 Unported Licence.

the main radical in the solution. In addition, hydroxyl radical is also generated as the secondary radical in the reaction. In order to find the dominant radical species in the investigated process, scavenging tests were conducted in the presence of benzene and TBA. Benzene is considered as a scavenger for both hydroxyl ($k_{HO\cdot} = 7.8 \times 10^9$ L mol^{-1} s^{-1})[50] and sulfate radicals ($k_{SO_4\cdot} = 2.4 \times 10^9$ L mol^{-1} s^{-1}).[51] Therefore, it can effectively quench both hydroxyl and sulfate radicals in the solution. On the other hand, TBA is a well-known hydroxyl radical scavenger, and the second order rate constant of TBA with hydroxyl radical ($k_{HO\cdot} = 3.8 \times 10^8$ to 7.6×10^8 L mol^{-1} s^{-1}) is higher than that of sulfate radical ($k_{SO_4\cdot} = 4 \times 10^5$ to 9.1×10^5 L mol^{-1} s^{-1}).[14,35] As it is shown in Fig. 6a, only a slight reduction of 17% in AMX removal rate was observed in the presence of 50 mM of TBA, while about 73% reduction was observed in the presence of benzene. The higher reduction rate in removal efficiency clearly indicates that sulfate radicals as the main radical species are quenched in the reaction. Similar studies have also been conducted and proved that sulfate radical is the main radical species in the UV/PS process. Ding *et al.*[52] investigated the performance of UV/PS process for the degradation of Rhodamine B dye. They used methanol and TBA as sulfate and hydroxyl radical quenchers, respectively. The scavenging experiments have also proved that a negligible amount of hydroxyl radical is generated in the UV/PS process.

The rate constants of pollutant removal with and without $SO_4^{\cdot -}$ scavengers could be used for the calculation of relative contribution of $SO_4^{\cdot -}$ and $HO^{\cdot}$ in the sulfate-based AOPs (eqn (6) and (7)).[53]

$$HO^{\cdot}\ \text{contribution}\ (\%) = \frac{k_{obs}\ \text{with}\ HO^{\cdot}\ \text{scavenger}}{k_{obs}\ \text{without scavenger}} \times 100 \quad (6)$$

$$SO_4^{\cdot -}\ \text{contribution}\ (\%) = 100 - HO^{\cdot}\ \text{contribution}\ (\%) \quad (7)$$

Considering the negligible removal of AMX by UV radiation and also lower reaction rate of the selected scavengers with the secondary radical species (10^{-3} L mol^{-1} s^{-1})[54] and the reaction rate constants obtained in Fig. 4, it is found that almost 91.8% of the AMX oxidation is due to the generation of $SO_4^{\cdot -}$ and 8.2%

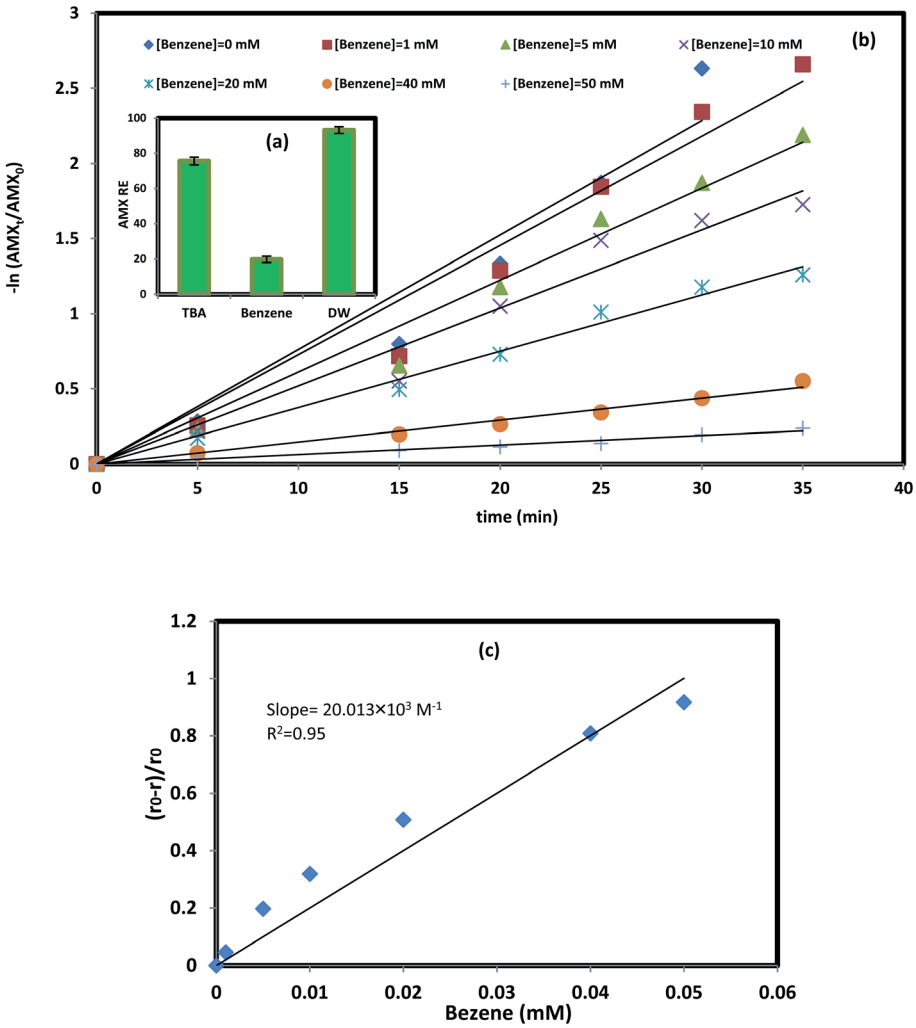

Fig. 6 (a) AMX degradation in the presence of 50 mM radical quenchers, (b) AMX (50 mg L^{-1}) degradation kinetics in the presence of various benzene concentrations, and (c) Stern–Volmer type plot.

© 2022 The Author(s). Published by the Royal Society of Chemistry

Open Access Article. Published on 18 May 2022. Downloaded on 12/27/2025 9:06:54 AM.
This article is licensed under a Creative Commons Attribution-NonCommercial 3.0 Unported Licence.

is due to the HO$^{\bullet}$. Therefore, it can be deduced that both sulfate and hydroxyl radicals are the main oxidizing agents in the UV/PS system.

3.6. Calculation of the second-order rate constant of sulfate radical with AMX

Completion kinetic using benzene was applied to measure the rate constant of sulfate radical with AMX. The reaction rate constant of benzene with sulfate radical is reported to be 2.4×10^9 L mol^{-1} s^{-1}.[51] The presence of various concentrations of benzene in the UV/PS process showed a significant reduction in AMX removal efficiency. Considering the point that there is a competition between AMX and benzene in the solution to react with sulfate radical and the known reaction rate of benzene with sulfate radical, the reaction rate of AMX with sulfate radical can be calculated. In the UV/PS process with benzene as the scavenger, the following reactions are assumed to take place:

$$\text{AMX} + \text{SO}_4^{\bullet -} \rightarrow \text{products } r_1 = k_1[\text{AMX}][\text{SO}_4^{\bullet -}] \quad (8)$$

$$\text{Benzene} + \text{SO}_4^{\bullet -} \rightarrow \text{products } r_2 = k_2[\text{benzene}][\text{SO}_4^{\bullet -}] \quad (9)$$

Accordingly, the overall reaction rate of sulfate radical (r) is as follow:

$$r = [\text{SO}_4^{\bullet -}] \times (k_1[\text{AMX}] + k_2[\text{benzene}]) \quad (10)$$

The AMX reaction rate in the absence of scavenger (r_1^0) can also be calculated based on the following equation:

$$\text{AMX} + \text{SO}_4^{\bullet -} \rightarrow \text{products } r_1^0 = k_1[\text{AMX}][\text{SO}_4^{\bullet -}] \quad (11)$$

It is assumed that the sulfate radical concentration in both reactions (eqn (8) and (9)) is the same in and the sulfate radical is the main oxidizing agent. Accordingly, the following equation could be developed:

$$r_1 = r\frac{k_1[\text{AMX}]}{k_1[\text{AMX}] + k_2[\text{benzene}]} \quad (12)$$

Fig. 6b illustrates the ln(AMX/AMX$_0$) *vs.* time at various benzene concentrations. The slope of the plots illustrates the reaction constant rate of the AMX as a function of benzene concentrations. Fig. 6c shows the $(r_1^0 - r_1)/r_1$ as a function of benzene concentration, which is a simple Stern–Volmer type plot. Therefore, the slope of the plot (20.013×10^3 M^{-1}) equals to k_2/k_1[AMX]. Consequently, the second-order rate constant of AMX with sulfate radical is calculated to be 8.56×10^9 L mol^{-1} s^{-1}.[3] Investigated the PS/Fe^{2+} process for AMX degradation and used the same method for calculation of the reaction rate constant of AMX with sulfate radical. They also found the reaction rate constant of the same order of magnitude.

$$\frac{(r_1^0 - r_1)}{r_1} = \frac{k_2[\text{benzene}]}{k_1[\text{AMX}]} \quad (13)$$

3.7. The effect of anions

Water matrix and the presence of various organic and anions in the AOPs may deteriorate process performance. Accordingly, AMX degradation was investigated in the presence of humic acid (simulation of NOM) and inorganic anions. Environmentally relevant concentrations of the water matrix were spiked into the solution. Fig. 7 illustrates the results of the water matrix effect on AMX degradation. As shown in the figure, humic acid had the highest adverse effect on process performance, and almost 26% reduction was observed in the presence of 10 mg L^{-1} of humic acid. This reduction could be attributed to the scavenging capability of humic acid in AOPs. Although the reaction rate constant of NOM with sulfate radical ($k_{\text{SO}_4^{\bullet -},\text{NOM}} = 6 \times 10^6$ M^{-1} s^{-1}) is lower than that AMX with sulfate radical, it can partially quench the sulfate radical.[55] On the other hand, considering the point that almost 8% of AMX degradation in UV/PS was attributed to the hydroxyl radical (Section 3.6) and the reaction rate of NOM with hydroxyl radical ($k_{\text{HO}^{\bullet},\text{NOM}} = 2.23 \times 10^8$ M^{-1} s^{-1}),[56] the AMX removal efficiency is consequently expected to drop in the presence of humic acid. The results also show that almost 16% reduction occurred in the presence of nitrate. The inhibition effect of nitrate in the UV-based AOPs could be due to the absorbance of the UV light by nitrate. Nitrate suppresses both direct photolysis of AMX and mainly persulfate activation leading to reduction of sulfate radical formation and process efficiency.[57] Carbonate also shows a relatively higher reduction in removal efficiency. Carbonate is able to quench radical species leading the reduction of the target reaction rate. The interaction of carbonate with$\text{SO}_4^{\bullet -}$[58] and HO$^{\bullet}$[59] resulted in the formation of carbonate radical as given in the following equations:

$$\text{CO}_3^{2-} + \text{SO}_4^{\bullet -} \rightarrow \text{CO}_3^{\bullet 2-} + \text{SO}_4^{\bullet -} \quad (14)$$

$$\text{CO}_3^{2-} + \text{HO}^{\bullet} \rightarrow \text{CO}_3^{\bullet 2-} + \text{H}_2\text{O} \quad (15)$$

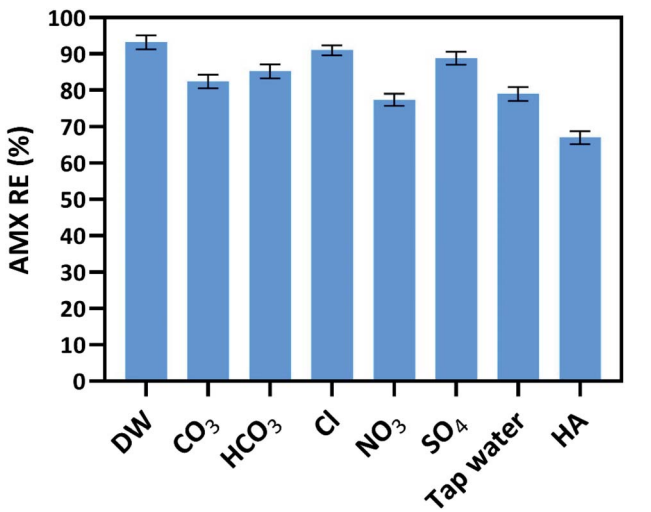

Fig. 7 The effect of water matrix on AMX degradation ([humic acid] = 10 mg L^{-1}, [anions] = 100 mg L^{-1}).

© 2022 The Author(s). Published by the Royal Society of Chemistry

Open Access Article. Published on 18 May 2022. Downloaded on 12/27/2025 9:06:54 AM. This article is licensed under a Creative Commons Attribution-NonCommercial 3.0 Unported Licence.

Table 1 Economic comparison of UV, UV/PS, H_2O_2/PS, US/PS, and heat/PS processes[a]

	Electrical energy cost ($\$m^{-3}$ per order)	Chemical cost ($\$m^{-3}$ per order)	Total cost ($\$m^{-3}$ per order)
UV/PS	1.8	0.11	1.9
UV	96.6	0.00	96.6
H_2O_2/PS	323.4	0.13	323.5
Heat/PS	405.5	0.11	405.6
US/PS	205.5	0.11	205.6

[a] AMX initial concentration: 50 mg L^{-1}. Costs: PS ($0.18 mol^{-1}); H_2O_2 ($0.051 mol^{-1}); electricity: (0.11 \$ kW^{-1} h^{-1}).[63] Power: UV lamp (9 W); heater (500 W); stirrer (500 W); ultrasound (300 W).

Although organic compounds may be degraded by carbonate radical ($E_0 = 1.78$ V at pH 7),[60] it is not as strong oxidant as $SO_4^{\bullet-}$ and $HO^{\bullet}$. Therefore, reduction in the AMX removal efficiency is observed in the presence of carbonate.

The AMX degradation in the presence of chloride is negligible, and almost the same removal efficiency with distilled water has been reached. Presence of chloride ions along with sulfate radical leads to the generation of other chloride-based radicals such as $CLOH^{\bullet-}$, $Cl^{\bullet}$, and $Cl_2^{\bullet}$. Although the chloride-based radicals are less reactive than sulfate and hydroxyl radicals, it has been reported that $Cl_2^{\bullet}$ is able to attack the sulfur atom in the beta-lactam ring of the antibiotics.[61] Therefore, the scavenging effect of chloride in the UV/PS process for AMX degradation is negligible.

3.8. Cost analysis

An economic indicator was calculated based on the electrical energy and the oxidant costs to evaluate the cost-effectiveness of UV/PS compared to UV, H_2O_2/PS, US/PS, and heat/PS methods. Electric energy per order (E_{EO}), as the economic indicator, was calculated using the following equation:[62]

$$E_{EO}\left(\text{kW h m}^{-3}\text{ per order}\right) = \frac{Pt1000}{V\log\left(\frac{C_i}{C_f}\right)} = \frac{38.4P}{Vk_1} \quad (16)$$

where P is the power output (kW) of the UV lamp, stirrer, or heater; t is the irradiation, stirring, or heating time (h); V is the reactor volume (L); k_1 is the first-order rate constant (min^{-1}); C_i and C_f are initial and final concentrations of antibiotics, respectively. The total cost per order (E_{EO}^{total}) was calculated using the following equation:

$$E_{EO}^{total}\ (\$m^{-3}\text{ per order}) = E_{EO} \times \text{electricity cost } (\$\ kW^{-1}\ h^{-1}) + \text{chemical cost} \quad (17)$$

Generally, the major portion of the total cost of all processes is related to electrical energy cost (Table 1). Despite the lower removal efficiency of the UV process (without PS), its E_{EO}^{total} value is lower than H_2O_2/PS, US/PS, and heat/PS processes due to lower energy consumption of UV lamp compared to heater or stirrer. However, the cost of the UV process significantly decreased from 96.6 to 1.9 $\$m^{-3}$ per order by adding PS to the solution, leading to a higher rate constant of UV/PS process (0.084 min^{-1}) compared to the UV process (0.002 min^{-1}). Overall, the addition of PS to the UV photolysis process can both decrease the treatment cost and shorten the required time for degrading AMX.

3.9. Toxicity assessment

The cytotoxic effects of AMX on the viability of the HEK 293 cell lines are presented as percent cell viability in Fig. 8. The

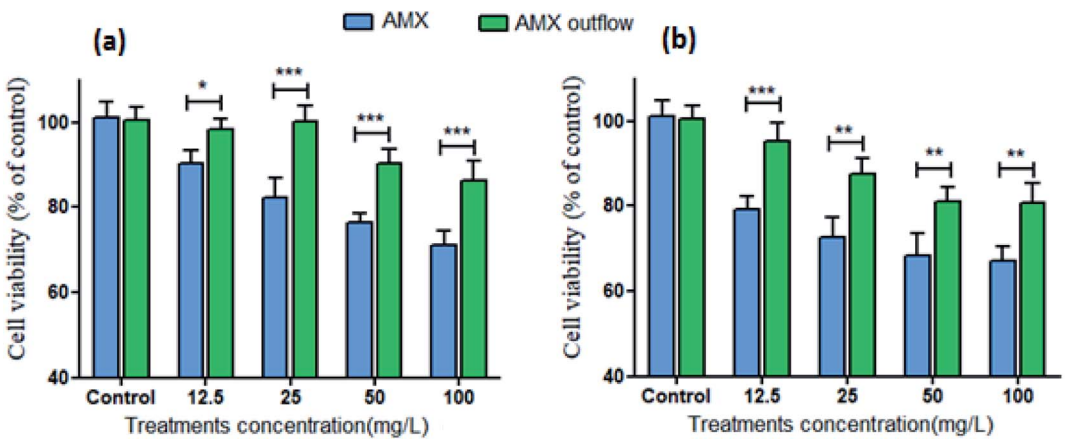

Fig. 8 Cytotoxicity assessment by MTT assay in HEK 293T cells following the exposure of various concentrations of AMX inflow and AMX outflow for 24 h (a) and 48 (b).

© 2022 The Author(s). Published by the Royal Society of Chemistry

Open Access Article. Published on 18 May 2022. Downloaded on 12/27/2025 9:06:54 AM.
This article is licensed under a Creative Commons Attribution-NonCommercial 3.0 Unported Licence.

Cytotoxicity results obtained from MTT assay showed that AMX inhibited the viability of HEK 293T cells in comparison to the control cell. As shown in the figure, a statistically significant decrease in percent cell viability (% control) was initiated following treatment of cells by AMX in 24 h and 48 h. The percentage of cell viability treated with AMX inflow was significantly lower than AMX outflow treated cells, and AMX inflow is more toxic in all concentrations. Therefore, it is concluded that the UV/PS process can significantly reduce the AMX-induced cell cytotoxicity due to the conversion of AMX to less toxic by-products. The results obtained in the identification of degradation by-products are confirming this fact that after treatment of the AMX-laden wastewater with generated radical species, the remaining products are not toxic. That's why, the HEK 293 cell which very sensitive cells for toxic compounds survive after exposure with the process effluent. Trovó *et al.*[64] investigated the photo-Fenton process for degradation of AMX, they also conducted the toxicity assessment by commercial bioassays, BiofixLumi-10, based on inhibition of the luminescence emitted by the marine bacteria *Vibrio fischeri*, and *Daphnia magna* immobilization. It is reported that the no significant change in the toxicity of 50 mg L^{-1} of AMX was observed by *Vibrio fischeri*. The inhibition of mobility of the neonates after 240 min of reaction time has been reported to be 45%. Comparing the results with our study also indicates that UV/PS process was more reliable than the photo-fenton process for AMX detoxification. In the similar condition with AMX concentration of 50 mg L^{-1} cell viability of about 90% and 802% percent were reached after 24 h and 48 h, respectively.

4. Conclusion

The present study thoroughly investigates the persulfate activation by different methods for degradation of antibiotics and comprehensive investigations are conducted to better understand and develop the methods. The effects of various operational parameters along with kinetic studies were conducted to better understand the degradation mechanisms for AMX degradation. In addition, the effectiveness of the process for AMX detoxification was also carried out by investigation of viability of the HEK 293 cells. It was found that persulfate activation by UV radiation is much more efficient than US, heat, and H_2O_2, and the solution pH played an important role for each process. The results show that acidic condition is favorable for AMX degradation in the UV/PS, heat/PS, and US/PS, while H_2O_2/PS process is not dependent on the solution pH. LC/MS analysis revealed that two potential degradation pathways of hydroxylation and the opening of the β-lactam ring could better explain the degradation pathway of AMX. The radical quenching tests with various scavengers were introduced into the reaction and it was fund that sulfate radical was the main oxidizing agent in the UV/PS process, while other radical species such as hydroxyl radicals are also generated. Experiments were also conducted to reach data for calculation of competition kinetics, and calculation showed that the second-order rate constant of AMX with sulfate radical is 8.56×10^9 L mol^{-1} s^{-1} which is close to the values reported in literature. The results of present study were also used for the cost analysis, it shows that that a total cost of 1.9 $\$m^{-3}$ per order is required in the UV/PS process which makes the proposed process an economic one. To better prove the reliability of the process for detoxification of the AMX, cytotoxicity of the process effluent was investigated and the results show that toxicity of the AMX solution was significantly reduced after degradation of AMX in the UV/PS process. Finally, it can be deduced that UV/PS process is an effective process for AMX degradation and detoxification.

Conflicts of interest

There are no conflicts to declare.

Acknowledgements

The authors would like to acknowledge the financial support of Maragheh University of Medical Sciences for this research under grant number 97 DAY18-PAM02.

References

1 J. Wang and S. Wang, *Chem. Eng. J.*, 2018, **334**, 1502–1517.
2 A. Eslami, A. Asadi, M. Meserghani and H. Bahrami, *J. Mol. Liq.*, 2016, **222**, 739–744.
3 R. Matta, H. Younes, R. Hanna, J. Saab and R. Abou-Khalil, *J. Environ. Manage.*, 2019, **245**, 375–383.
4 X. Bian, Y. Xia, T. Zhan, L. Wang, W. Zhou, Q. Dai and J. Chen, *Chemosphere*, 2019, **233**, 762–770.
5 Y. Zhang, Y. Xiao, Y. Zhong and T.-T. Lim, *Chem. Eng. J.*, 2019, **372**, 420–428.
6 M. Verma and A. K. Haritash, *J. Environ. Chem. Eng.*, 2019, **7**, 102886.
7 A. R. Mahmood, H. H. Al-Haideri and F. M. Hassan, *Adv. Public Health*, 2019, **2019**, 7851354.
8 F. Schreiber and U. Szewzyk, *Aquat. Toxicol.*, 2008, **87**, 227–233.
9 I. A. Alaton, S. Dogruel, E. Baykal and G. Gerone, *J. Environ. Manage.*, 2004, **73**, 155–163.
10 B. L. Phoon, C. C. Ong, M. S. Mohamed Saheed, P.-L. Show, J.-S. Chang, T. C. Ling, S. S. Lam and J. C. Juan, *J. Hazard. Mater.*, 2020, **400**, 122961.
11 I. C. Iakovides, I. Michael-Kordatou, N. F. F. Moreira, A. R. Ribeiro, T. Fernandes, M. F. R. Pereira, O. C. Nunes, C. M. Manaia, A. M. T. Silva and D. Fatta-Kassinos, *Water Res.*, 2019, **159**, 333–347.
12 H. Wang, W. Shi, D. Ma, Y. Shang, Y. Wang and B. Gao, *Chem. Eng. J.*, 2020, **392**, 123701.
13 F. J. Benitez, J. L. Acero, F. J. Real, G. Roldan and F. Casas, *Chemosphere*, 2011, **85**, 1430–1437.
14 G. Moussavi, M. Pourakbar, E. Aghayani and M. Mahdavianpour, *Chem. Eng. J.*, 2018, **350**, 673–680.
15 S. G. Poulopoulos, G. Ulykbanova and C. J. Philippopoulos, *Environ. Technol.*, 2020, 1–9, DOI: **10.1080/09593330.2020.1720300**.
16 M. L. Tran, C.-C. Fu and R.-S. Juang, *Environ. Sci. Pollut. Res.*, 2019, **26**, 11846–11855.

© 2022 The Author(s). Published by the Royal Society of Chemistry

Open Access Article. Published on 18 May 2022. Downloaded on 12/27/2025 9:06:54 AM. This article is licensed under a Creative Commons Attribution-NonCommercial 3.0 Unported Licence.

17 F. S. Souza, V. V. da Silva, C. K. Rosin, L. Hainzenreder, A. Arenzon and L. A. Féris, *Environ. Technol.*, 2018, **39**, 549–557.
18 M. Pirsaheb, H. Hossaini and H. Janjani, *Microchem. J.*, 2020, **153**, 104430.
19 M. Pourakbar, G. Moussavi and S. Shekoohiyan, *Ecotoxicol. Environ. Saf.*, 2016, **125**, 72–77.
20 J. H. Ramírez-Franco, L.-A. Galeano and M.-A. Vicente, *J. Environ. Chem. Eng.*, 2019, **7**, 103274.
21 A. Behnami, J.-P. Croué, E. Aghayani and M. Pourakbar, *RSC Adv.*, 2021, **11**, 36965–36977.
22 K. A. Rickman and S. P. Mezyk, *Chemosphere*, 2010, **81**, 359–365.
23 S. B. Shuchi, M. B. K. Suhan, S. B. Humayun, M. E. Haque and M. S. Islam, *J. Water Proc. Eng.*, 2021, **39**, 101690.
24 Y. Zhang, Y.-G. Zhao, F. Maqbool and Y. Hu, *J. Water Proc. Eng.*, 2022, **45**, 102496.
25 P. S. Bhandari, B. P. Makwana and P. R. Gogate, *J. Water Proc. Eng.*, 2020, **36**, 101316.
26 R. A. Fallahzadeh, M. H. Ehrampoush, M. Nabi Meybodi, M. T. Ghaneian, A. Dalvand, F. Omidi, M. H. Salmani, H. Fallahzadeh and A. H. Mahvi, *Korean J. Chem. Eng.*, 2020, **37**, 969–977.
27 S. F. Castilla-Acevedo, L. A. Betancourt-Buitrago, D. D. Dionysiou and F. Machuca-Martínez, *J. Hazard. Mater.*, 2020, **392**, 122389.
28 M. Pirsaheb and N. Moradi, *RSC Adv.*, 2020, **10**, 7396–7423.
29 S. Su, W. Guo, C. Yi, Y. Leng and Z. Ma, *Ultrason. Sonochem.*, 2012, **19**, 469–474.
30 D.-M. Gu, C.-S. Guo, Q.-Y. Feng, H. Zhang and J. Xu, *Water*, 2020, 12.
31 E. S. Elmolla and M. Chaudhuri, *J. Hazard. Mater.*, 2010, **173**, 445–449.
32 A. H. Hilles, S. S. Abu Amr, R. A. Hussein, O. D. El-Sebaie and A. I. Arafa, *J. Environ. Manage.*, 2016, **166**, 493–498.
33 R. Zhang, P. Sun, T. H. Boyer, L. Zhao and C.-H. Huang, *Environ. Sci. Technol.*, 2015, **49**, 3056–3066.
34 C. Jiang, Y. Ji, Y. Shi, J. Chen and T. Cai, *Water Res.*, 2016, **106**, 507–517.
35 G. Moussavi, M. Pourakbar, E. Aghayani, M. Mahdavianpour and S. Shekoohyian, *Chem. Eng. J.*, 2016, **294**, 273–280.
36 E. Can-Güven, S. Yazici Guvenc and G. Varank, *J. Water Proc. Eng.*, 2021, **42**, 102202.
37 A. Ioannidi, O. S. Arvaniti, M.-C. Nika, R. Aalizadeh, N. S. Thomaidis, D. Mantzavinos and Z. Frontistis, *Chemosphere*, 2022, **287**, 131952.
38 C. Liang and H.-W. Su, *Ind. Eng. Chem. Res.*, 2009, **48**, 5558–5562.
39 M. Panizza, A. Dirany, I. Sirés, M. Haidar, N. Oturan and M. A. Oturan, *J. Appl. Electrochem.*, 2014, **44**, 1327–1335.
40 D. Kanakaraju, J. Kockler, C. A. Motti, B. D. Glass and M. Oelgemöller, *Appl. Catal., B*, 2015, **166–167**, 45–55.
41 A. V. Karim and A. Shriwastav, *Environ. Res.*, 2021, **200**, 111515.
42 M. L. Crimi and J. Taylor, *Soil Sediment Contam.*, 2007, **16**, 29–45.
43 J. Méndez-Díaz, M. Sánchez-Polo, J. Rivera-Utrilla, S. Canonica and U. von Gunten, *Chem. Eng. J.*, 2010, **163**, 300–306.
44 J. M. Monteagudo, A. Durán, R. González and A. J. Expósito, *Appl. Catal., B*, 2015, **176–177**, 120–129.
45 L. Liu, S. Lin, W. Zhang, U. Farooq, G. Shen and S. Hu, *Chem. Eng. J.*, 2018, **346**, 515–524.
46 J. M. Monteagudo, H. El-taliawy, A. Durán, G. Caro and K. Bester, *J. Hazard. Mater.*, 2018, **357**, 457–465.
47 L. Zhu, L. Lu, S. Wang, J. Wu, J. Shi, T. Yan, C. Xie, Q. Li, M. Hu and Z. Liu, in *Developing Solid Oral Dosage Forms*, ed. Y. Qiu, Y. Chen, G. G. Z. Zhang, L. Yu and R. V. Mantri, Academic Press, Boston, 2nd edn, 2017, pp. 297–329, DOI: 10.1016/B978-0-12-802447-8.00011-X.
48 Q. Li, R. Jia, J. Shao and Y. He, *J. Cleaner Prod.*, 2019, **209**, 755–761.
49 T.-Y. Tan, Z.-T. Zeng, G.-M. Zeng, J.-L. Gong, R. Xiao, P. Zhang, B. Song, W.-W. Tang and X.-Y. Ren, *Sep. Purif. Technol.*, 2020, **235**, 116167.
50 R. H. Schuler and G. Albarran, *Radiat. Phys. Chem.*, 2002, **64**, 189–195.
51 P. Warneck and J. Ziajka, *Bunsen-Ges. Phys. Chem.*, 1995, **99**, 59–65.
52 X. Ding, L. Gutierrez, J.-P. Croue, M. Li, L. Wang and Y. Wang, *Chemosphere*, 2020, **253**, 126655.
53 Y. Zhang, Q. Zhang and J. Hong, *Appl. Surf. Sci.*, 2017, **422**, 443–451.
54 G. P. Anipsitakis and D. D. Dionysiou, *Environ. Sci. Technol.*, 2004, **38**, 3705–3712.
55 P. Westerhoff, S. P. Mezyk, W. J. Cooper and D. Minakata, *Environ. Sci. Technol.*, 2007, **41**, 4640–4646.
56 P. M. D. Gara, G. N. Bosio, M. C. Gonzalez, N. Russo, M. del Carmen Michelini, R. P. Diez and D. O. Mártire, *Photochem. Photobiol. Sci.*, 2009, **8**, 992–997.
57 J. Peng, G. Wang, D. Zhang, D. Zhang and X. Li, *J. Photochem. Photobiol., A*, 2016, **326**, 9–15.
58 H. Gao, J. Chen, Y. Zhang and X. Zhou, *Chem. Eng. J.*, 2016, **306**, 522–530.
59 G. V. Buxton, C. L. Greenstock, W. P. Helman and A. B. Ross, *J. Phys. Chem. Ref. Data*, 1988, **17**, 513–886.
60 Y. Liu, X. He, Y. Fu and D. D. Dionysiou, *J. Hazard. Mater.*, 2016, **305**, 229–239.
61 L. Szabó, T. Tóth, E. Takács and L. Wojnárovits, *J. Photochem. Photobiol., A*, 2016, **326**, 50–59.
62 J. R. Bolton, K. G. Bircher, W. Tumas and C. A. Tolman, *Pure Appl. Chem.*, 2001, **73**, 627–637.
63 Y. Xiao, L. Zhang, W. Zhang, K. Y. Lim, R. D. Webster and T. T. Lim, *Water Res.*, 2016, **102**, 629–639.
64 A. G. Trovó, R. F. Pupo Nogueira, A. Agüera, A. R. Fernandez-Alba and S. Malato, *Water Res.*, 2011, **45**, 1394–1402.

© 2022 The Author(s). Published by the Royal Society of Chemistry